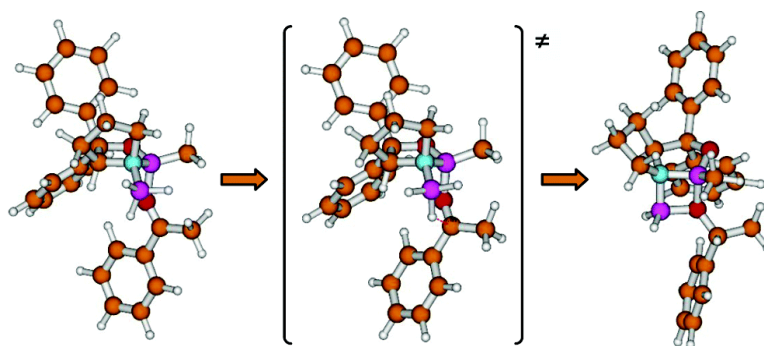


## Quantum Mechanical Study of Stereoselectivity in the Oxazaborolidine-Catalyzed Reduction of Acetophenone

Giuliano Alagona, Caterina Ghio, Maurizio Persico, and Simone Tomasi

*J. Am. Chem. Soc.*, **2003**, 125 (33), 10027-10039 • DOI: 10.1021/ja034928d • Publication Date (Web): 23 July 2003

Downloaded from <http://pubs.acs.org> on March 29, 2009



### More About This Article

Additional resources and features associated with this article are available within the HTML version:

- Supporting Information
- Links to the 3 articles that cite this article, as of the time of this article download
- Access to high resolution figures
- Links to articles and content related to this article
- Copyright permission to reproduce figures and/or text from this article

[View the Full Text HTML](#)

## Quantum Mechanical Study of Stereoselectivity in the Oxazaborolidine-Catalyzed Reduction of Acetophenone

Giuliano Alagona,<sup>\*,†</sup> Caterina Ghio,<sup>†</sup> Maurizio Persico,<sup>‡</sup> and Simone Tomasi<sup>‡</sup>

Contribution from the Istituto per i Processi Chimico-Fisici, CNR, Via Moruzzi 1, I-56124 Pisa, Italy, and Dipartimento di Chimica e Chimica Industriale, Università di Pisa, Via Risorgimento 35, I-56126 Pisa, Italy

Received February 28, 2003; E-mail: G.Alagona@ipcf.pi.cnr.it

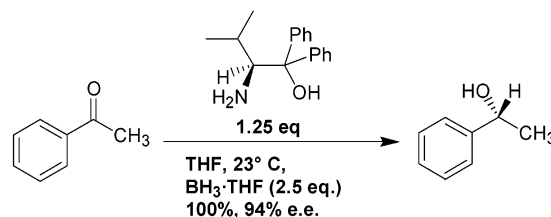
**Abstract:** Chiral oxazaborolidines, known as CBS catalysts after the work of Corey, Bakshi and Shibata, are used for the stereoselective reduction of prochiral ketones to secondary chiral alcohols. Due to their relative low cost, ease of use, and high selectivity, their popularity has remarkably grown in the last 15 years. Oxazaborolidine-catalyzed reductions have been much studied, both experimentally and computationally, by means of semiempirical methods. Though, a more accurate high level quantum mechanical study on the complete system, capable of elucidating reliably the origins of stereoselectivity, is still lacking. Therefore, the acetophenone (PhMK) reduction with Corey's oxazaborolidine has been modeled for the first time with ab initio and DFT-B3LYP calculations on the complete system as well as with AM1. Calculations on the complexation of BH<sub>3</sub> to CBS, which can occur only in a cis fashion with respect to the hydrogen on the stereogenic C-4 carbon atom, have allowed us to confirm the great rigidity of Corey's catalyst, possibly determining its excellent enantioselectivity. Acetophenone–CBS–BH<sub>3</sub> complexes were characterized at various levels of theory, and it was found that the picture obtained depends heavily on the method adopted. A computational strategy for identifying the hydride transfer transition states of the competing pathways was developed and tested, using a model system for which the transition state geometry was already known. The application of the TS search method to the reduction of acetophenone allowed the characterization of the TS's for the competing pathways in this reaction, making it possible to predict with good quantitative accuracy the stereochemical outcome of the reaction at all the levels of theory adopted. The characterization of the intermediate oxazadiboretane products confirmed that the highly exothermic hydride transfer provides the thermodynamical drive for the reaction.

### Introduction

In the past decades, numerous methodologies for the stereoselective reduction of carbonyl compounds with boron and aluminum hydrides have been developed, based on chiral reducing reagents or achiral ones, in the presence of chiral catalysts.<sup>1</sup>

Research done in the first half of the 1980s by Itsuno and co-workers led to the discovery of a reagent obtained from the reaction of borane with stereochemically pure (*S*)-2-amino-3-methyl-butanol, derived from valine, in defined ratios. The reagent, used in a slight excess with respect to the stoichiometry of the reaction, was capable of reducing with excellent yields and good enantiomeric excesses a great variety of prochiral ketones, and particularly arylalkyl ketones (see Scheme 1).<sup>2–5</sup> Itsuno's group subsequently modified the structure of the reagent

**Scheme 1.** Reduction of Prochiral Ketones with Itsuno's Reagent



by introducing two phenyl groups on the hydroxyl carbon atom, thus improving its efficiency.

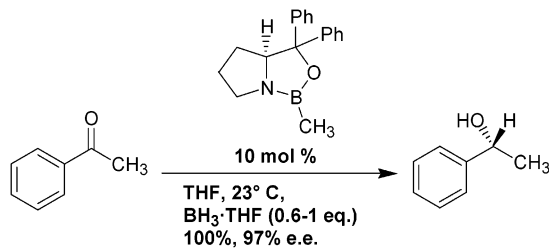
In 1987–88, Corey, Bakshi, and Shibata constructed a new class of structurally rigid oxazaborolidines, which they used in catalytic quantity for the reduction of prochiral ketones, and defined the reducing species, proposing for the first time that the reducing agent is an oxazaborolidine, as well as its mechanism of action.<sup>6–8</sup> The second generation oxazaborolidine by Corey, Bakshi, and Shibata is capable of reducing a great

<sup>†</sup> CNR.

<sup>‡</sup> Università di Pisa.

- (1) Corey, E. J.; Helal, P. J. *Angew. Chem., Int. Ed.* **1998**, *37*, 1986–2012.
- (2) Hirao, A.; Itsuno, S.; Nakahama, S.; Yamazaki, N. *J. Chem. Soc., Chem. Commun.* **1981**, 315–317.
- (3) Itsuno, S.; Hirao, A.; Nakahama, S.; Yamazaki, N. *J. Chem. Soc., Perkin Trans. 1* **1983**, 1673–1676.
- (4) Itsuno, S.; Hirao, A.; Nakahama, S.; Yamazaki, N. *J. Chem. Soc., Chem. Commun.* **1983**, 469–470.
- (5) Itsuno, S.; Nakano, M.; Miyazaki, K.; Masuda, H.; Ito, K.; Hirao, A.; Nakahama, S. *J. Chem. Soc., Perkin Trans. 1* **1985**, 2039–2044.

- (6) Corey, E. J.; Bakshi, R. K.; Shibata, S. *J. Am. Chem. Soc.* **1987**, *109*, 5551–5553.
- (7) Corey, E. J.; Bakshi, R. K.; Shibata, S.; Chen, C.-P.; Singh, V. K. *J. Am. Chem. Soc.* **1987**, *109*, 7925–7926.
- (8) Corey, E. J.; Bakshi, R. K.; Shibata, S. *J. Org. Chem.* **1988**, *53*, 2861–2863.

**Scheme 2.** Reduction of Prochiral Ketones with Corey's Catalyst**Table 1.** Stereoselectivity of the Reductions Carried out with Corey's Catalyst<sup>a</sup>

R <sub>1</sub>	R <sub>2</sub>	ee %
Ph	Me	97
Ph	Et	96.7
Ph	CH <sub>2</sub> Cl	95.3
<i>t</i> -Bu	Me	97.3
<i>c</i> -Hex	Me	84
tetrahydronaphthalene-1-one	tetrahydronaphthalene-1-one	86

<sup>a</sup> Data from ref 7.

variety of ketones under mild reaction conditions, with quantitative yields and excellent enantiomeric excesses (see Scheme 2 and Table 1). Moreover, the CBS catalyst (so-called after the names of its inventors) bearing a methyl substituent at the endocyclic boron shows a superior stability, allowing it to be weighed in the open air.

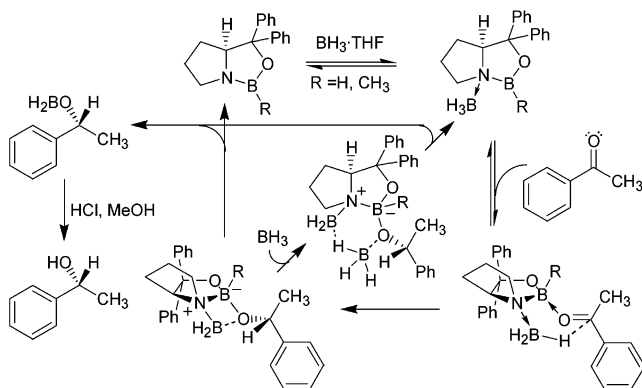
Eventually, X-ray diffraction measurements done in Corey's group confirmed that the reducing agent is really an oxazaborolidine and that borane coordinates to it through the nitrogen atom.<sup>1,9</sup>

The CBS catalyst offers positive results with a wide variety of polyfunctional ketones, making this methodology very useful in several fields of organic synthesis, like those of natural organic substances, chiral building blocks, and bioactive compounds. Application of the oxazaborolidine-catalyzed asymmetric reduction was eventually extended to imines and oximes,<sup>5,10–12</sup> to afford chiral amines or hydroxylamines.

**Mechanism of the Oxazaborolidine-Catalyzed Ketone Reduction.** The general mechanistic model proposed by Corey and co-workers for the enantioselective reduction of ketones with BH<sub>3</sub> in the presence of oxazaborolidines as chiral catalysts explains the role of the structural characteristics of the catalyst in determining the absolute configuration of the product, the excellent enantioselectivity of the reaction, its exceptional rate enhancement, and the turnover of the catalyst.

The catalytic cycle (Scheme 3) can be summarized in four principal steps: (1) coordination of borane to the catalyst, (2) complexation of the ketone to the endocyclic boron via Lewis acid–base interaction, (3) hydride transfer to the carbonyl carbon, (4) dissociation of an alkoxyborane moiety and regeneration of the catalyst.

The initial step is very rapid and probably reversible. BH<sub>3</sub> coordinates to the Lewis base nitrogen atom cis to the hydrogen on the carbon (C-4) of the ring fusion. Coordination in a trans

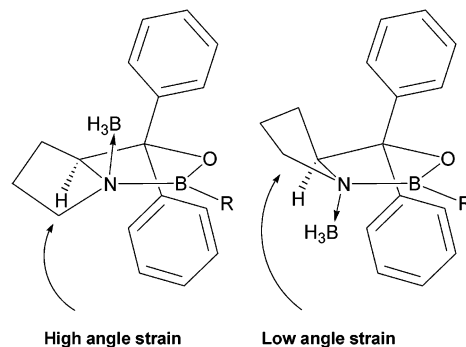
**Scheme 3.** Catalytic Cycle of the CBS Reduction<sup>1</sup>

way, leading to the opposite enantiomer, would imply that the proline ring assumes a high energy twisted conformation (see Figure 1). The presence of a rigid, fused ring system is thus important for high enantioselectivity. When the fused ring system is absent, like in Itsuno's oxazaborolidine derived from diphenylvalinol, trans coordination is to some extent possible, leading to a slightly lowered enantioselectivity (see Scheme 4).

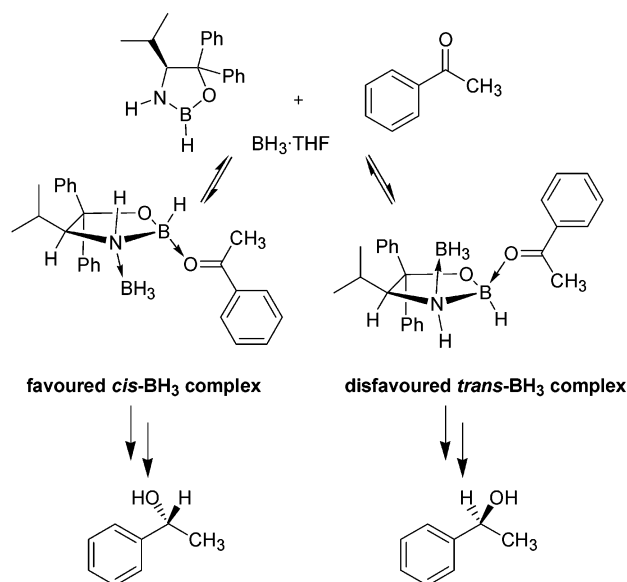
Unambiguous support for the initial coordination step comes from the observation by <sup>11</sup>B NMR spectroscopy that the oxazaborolidine and borane form a 1:1 complex and from the fact that crystalline R–CBS–BH<sub>3</sub> (R = Me) has been isolated and structurally defined by X-ray diffraction analysis.

The next step is the formation of a Lewis acid–base complex between the ketone, for example, acetophenone (PhMK) and the CBS–BH<sub>3</sub> complex. The ketone binds with its more sterically accessible lone pair cis to the coordinated BH<sub>3</sub>, which is the only possible way because the other face of the oxazaborolidine is virtually blocked by the rigid proline ring and by the phenyl group cis to it.

There are two consequences produced by this manner of binding. The first is that electron density is shifted from the carbonyl bond to the endocyclic boron, effectively making the carbonyl carbon more susceptible to hydride attack. The second is that the electronically deficient carbonyl carbon and the coordinated BH<sub>3</sub> are aligned for a stereoelectronically favorable, face-selective hydride transfer via a six-membered transition state. Thus, the coordination of BH<sub>3</sub> and of the ketone to the oxazaborolidine has a synergic effect enhancing the reactivity of both partners, in the best geometrical condition for the hydride transfer to happen, while making the catalyzed reduction much faster than the corresponding noncatalyzed one.

**Figure 1.** Difference between the trans and cis coordination of BH<sub>3</sub> to CBS relative to the hydrogen on the carbon (C-4) of the ring fusion. The trans compound is destabilized compared to the cis because of the highly strained conformation of the proline ring.<sup>13</sup>

- (9) Corey, E. J.; Azimioara, M.; Sarshar, S. *Tetrahedron Lett.* **1992**, *33*, 3429–3430.  
 (10) Itsuno, S.; Sakurai, S.; Ito, K.; Hirao, A.; Nakahama, S. *Bull. Chem. Soc. Jpn.* **1987**, *60*, 395–396.  
 (11) Sakito, Y.; Yoneyoshi, Y.; Suzukamo, G. *Tetrahedron Lett.* **1988**, *29*, 223–224.  
 (12) Tyllier, R. D.; Boudreau, C.; Tschäen, D.; Dolling, U.-H.; Reider, S. *Tetrahedron Lett.* **1995**, *36*, 4337.

**Scheme 4.** A Possible Reduction Pathway for Itsuno's Oxazaborolidine with Somewhat Lower Enantioselectivity<sup>1 a</sup>

<sup>a</sup> cis and trans indicate the spatial disposition between BH<sub>3</sub> and the hydrogen on C-4.

To answer the question whether the ketone complexation or the subsequent hydride transfer is the rate-limiting step, reduction rates of differently *p*-substituted acetophenone derivatives, containing electron-withdrawing and electron-donating groups, have been measured. In both cases, faster reduction rates were recorded, as compared with the reduction rate of unsubstituted acetophenone. Additional information was obtained by measuring the kinetic isotope effect for the hydride transfer.<sup>14</sup> The  $k_H/k_D$  ratio, 1.7, indicates an early transition state for the highly exothermic hydride transfer. So, according to experimental data, both ketone complexation and hydride transfer are probably fast and comparably rate-limiting.

It appears that the crucial steps for modeling stereoselectivity are the complexation of the substrate to CBS and the subsequent hydride transfer, which define the stereochemical outcome, which afterward cannot be any longer modified.

After the hydride transfer, an oxazadiboretane transient intermediate is formed. The existence of this species, supported also by semiempirical and ab initio calculations,<sup>15–19</sup> has been observed by <sup>11</sup>B NMR spectroscopy at low temperature (–50/–100 °C).<sup>20</sup> The reduction product can dissociate as an alkoxyborane from the transient oxazadiboretane via two possible reaction pathways: (2,2) cycloelimination, to regenerate the catalyst and form the alkoxyborane or addition of BH<sub>3</sub> to form a six-membered BH<sub>3</sub>-bridged species, which decomposes to the CBS–BH<sub>3</sub> complex and the alkoxyborane.

Up to two of the three hydrides of borane can be used during the reaction.<sup>8,21</sup> According to the explanation based on model

compounds proposed by Nevalainen,<sup>22</sup> the alkoxyborane moiety obtained reducing a molecule of ketone with the first hydride of BH<sub>3</sub> can coordinate with the B atom to the N of the oxazaborolidine and employ one of the two remaining hydrides for reduction of a second molecule of ketone. Formation of the CBS–alkoxyborane complex can occur by direct coordination of an alkoxyborane molecule to the N atom of the regenerated catalyst or by intramolecular rearrangement from the intermediate oxazadiboretane reduction product. Eventual formation of the CBS–dialkoxyborane complex would be not viable due to unfavorable steric interactions between the 5,5-diphenyl substituent and the alkyl groups of the dialkoxyborane moiety.<sup>16</sup> It has also been mentioned the possibility that two molecules of alkoxyborane disproportionate giving a molecule of dialkoxyborane and BH<sub>3</sub>.<sup>1</sup>

**Brief Survey of the Theoretical Work on Oxazaborolidines.** Despite the great interest for this reaction, theoretical work investigating the oxazaborolidine reduction of ketones started to appear in the literature only at the beginning of the past decade. In 1991–1996, Nevalainen studied small model systems with ab initio calculations,<sup>13,15,16,22–35</sup> from which he managed to extract some interesting mechanistic information confirming Corey's theories. For example, he could confirm Corey's statement that the free energy difference favoring cis BH<sub>3</sub> complexation over the trans one (with respect to the hydrogen on C-4) in the fused oxazaborolidines such as those derived from proline is much larger than in nonfused ring oxazaborolidines such as those derived from valine.<sup>13</sup> He also suggested that complexation modes different from exo/anti (see the following sections for definitions of ketone–oxazaborolidine complexes) are possible, though he did not realize the importance of the B–C–O–R<sub>L</sub> torsion in the generation of other possible complex geometries.<sup>25,26</sup> Furthermore, he provided a computational explanation for the formation of the dimeric aggregates between two molecules of oxazaborolidine, whose existence had been deduced from NMR experiments. Concerning this topic, he also supplied computational ground to the correct idea that, in Lewis basic solvents, like THF, oxazaborolidines dimerize with more difficulty.<sup>28,29</sup> Nevalainen also made a number of efforts to rationalize the mechanism, investigating the species involved after hydride transfer has occurred, thus identifying for the first time the oxazadiboretane species with a tentative explanation of how it is cleaved to afford the product and regenerate the catalyst.<sup>15,16,31,32</sup> However, despite his appreciable work, Nevalainen did not formulate a complete and precise rationale of enantioselection in oxazaborolidine reactions, because in his studies he focused on the characterization of

- (13) Nevalainen, V. *Tetrahedron: Asymmetry* **1992**, *3*, 1441–1453.  
 (14) Corey, E. J.; Link, J. O.; Bakshi, R. K. *Tetrahedron Lett.* **1992**, *33*, 7107–7110.  
 (15) Nevalainen, V. *Tetrahedron: Asymmetry* **1991**, *2*, 1133–1155.  
 (16) Nevalainen, V. *Tetrahedron: Asymmetry* **1992**, *3*, 921–932.  
 (17) Linney, L. P.; Self, C. R.; Williams, I. H. *J. Chem. Soc., Chem. Commun.* **1994**, 1651–1652.  
 (18) Li, M.; Tian, A. *THEOCHEM* **2001**, *544*, 37–47.  
 (19) Li, M.; Xie, R.; Hu, X.; Tian, A. *Int. J. Quantum Chem.* **2000**, *81*, 261–268.  
 (20) Douglas, A. W.; Tschaen, D. M.; Reamer, R. A.; Shi, Y.-J. *Tetrahedron: Asymmetry* **1996**, *7*, 1303–1308.

- (21) (a) Mathre, D. J.; Thompson, A. S.; Douglas, A. W.; Hoogsteen, K.; Carrol, J. D.; Corley, E. G.; Grabowski, E. J. *J. Org. Chem.* **1993**, *58*, 2880–2888. (b) Prasad, K. R. K.; Joshi, N. N. *Tetrahedron: Asymmetry* **1996**, *7*, 3147–3152. (c) Stone, G. B. *Tetrahedron: Asymmetry* **1994**, *5*, 465–472.  
 (22) Nevalainen, V. *Tetrahedron: Asymmetry* **1996**, *7*, 2655–2664.  
 (23) Nevalainen, V. *Tetrahedron: Asymmetry* **1991**, *2*, 63–74.  
 (24) Nevalainen, V. *Tetrahedron: Asymmetry* **1991**, *2*, 429–435.  
 (25) Nevalainen, V. *Tetrahedron: Asymmetry* **1992**, *3*, 1563–1572.  
 (26) Nevalainen, V. *Tetrahedron: Asymmetry* **1991**, *2*, 827–842.  
 (27) Nevalainen, V. *Tetrahedron: Asymmetry* **1992**, *3*, 933–945.  
 (28) Nevalainen, V. *Tetrahedron: Asymmetry* **1993**, *4*, 1505–1519.  
 (29) Nevalainen, V. *Tetrahedron: Asymmetry* **1993**, *4*, 1597–1602.  
 (30) Nevalainen, V. *Tetrahedron: Asymmetry* **1994**, *5*, 289–296.  
 (31) Nevalainen, V. *Tetrahedron: Asymmetry* **1994**, *5*, 903–908.  
 (32) Nevalainen, V. *Tetrahedron: Asymmetry* **1994**, *5*, 387–394.  
 (33) Nevalainen, V. *Tetrahedron: Asymmetry* **1994**, *5*, 395–402.  
 (34) Nevalainen, V. *Tetrahedron: Asymmetry* **1995**, *6*, 1431–1440.  
 (35) Qallich, G. J.; Blake, J. F.; Woodall, T. M. *J. Am. Chem. Soc.* **1994**, *116*, 8516–8525.



reaction intermediates rather than on transition states and because in his model systems solely symmetric carbonyl compounds were employed.

Only addressing a larger system, Blake, Quallich, and Woodall<sup>35</sup> gave theoretical ground to some of the hypotheses presented by Corey and co-workers. In their remarkable work (exceptional if considered that it was published in 1994), the authors demonstrate how enantiomeric excess depends on the extent to which the upper face of the oxazaborolidine is blocked for ketone complexation; or, to say it with their words, “molecular recognition of the borane and ketone carbonyl group by an appropriately substituted oxazaborolidine is the key element for enantioselectivity”. Their work is unique up to now, because an important part is devoted to the discussion of energetics and geometrical data of ab initio fully optimized transition states, which have not been reported elsewhere, even in more recent times. Blake, Quallich, and Woodall also observed that the calculated structures, their energies, and the existence of key intermediates are sensitive to the level of theory applied. In particular, they observed that no stable oxazaborolidine–ketone complexes were located with HF/6-31G\* optimizations. Using a different system, we made the same observation, and that was the major fact that prompted us to study the B–O interaction, as reported elsewhere.<sup>36</sup>

Apart from this work, the high computational costs of ab initio calculations involving real systems limited the study of oxazaborolidine reductions to semiempirical methods, such as MNDO or AM1,<sup>17,37–42</sup> which can support Corey’s mechanism to some extent, although they are not able to predict the stereochemical outcome of the reaction accurately.

In most cases, semiempirical calculations were used in support of experimental work, generally with the aim to develop new oxazaborolidines, more efficient toward specific classes of substrates.<sup>40,41</sup> In three cases, AM1<sup>39,41</sup> and MNDO<sup>37</sup> transition state characterizations succeeded in predicting the experimentally observed chirality. A particularly noteworthy work by Bringmann and co-workers relates the nondynamic kinetic resolution of configurationally stable biaryl lactones by an oxazaborolidine-catalyzed reduction, performed in the laboratory and described with AM1.<sup>39</sup> Another interesting study, by Linney, Self, and Williams, also conducted at the AM1 level, rather than exploring the origins of stereoselectivity, is devoted to the complete delineation of the species involved in the two competing pathways of the reduction of acetone, by the reconstruction of the intrinsic reaction coordinate.<sup>17</sup> The conclusions from this study are consistent with Nevalainen’s and more detailed, though obtained with a semiempirical method.

Recently Tian, Li, and co-workers studied some of the key species of the catalytic cycle by means of HF/6-31G\* calculations. The catalytic systems chosen for their work are close to CBS catalysts, with the difference that the two phenyl groups

in position 5 are replaced by two hydrogen atoms. In their studies of pinacolone reduction,<sup>18,43</sup> Tian and Li describe borane–catalyst–substrate ternary complexes and the oxazaborolidine species corresponding to the intermediate product from hydride transfer. No calculation is reported about transition states in those papers nor in those dealing with a modified CBS catalyst containing a sulfur atom instead of the central methylene unit of the proline ring (in this case as well, the 5,5′-diphenylic substituent is omitted).<sup>19,44–46</sup> This sulfur-containing modification to the classical CBS catalyst leads to complete inversion of stereoselectivity, as shown independently by three experimental groups.<sup>47–50</sup> A more detailed description, with full characterization of the transition states for the competing reaction pathways, would have been useful for explaining this interesting phenomenon.

The last paper from the Li–Tian groups describes the CBS reduction of keto-oximes similar to those reduced experimentally by Tillyer and co-workers,<sup>12</sup> though a smaller model was used for the computational work. In this case, B3LYP/6-31G\* calculations have been carried out on the system. While interesting conclusions are drawn on chemoselectivity, the considerations reported about the stereochemical outcome of the reaction are lacking of a more complete argumentation, since they are not supported by the transition states characterization.

From a perusal of published papers about the modeling of CBS reductions, it appears evident that, although important steps have been taken toward the understanding of stereoselectivity, a thorough high level quantum mechanical study is missing, covering also the detailed description of all the transition states involved, and performed on the whole system used experimentally. That investigation would be necessary to gain a reliable insight and predictive power into the stereochemistry of these reductions.

## Computational Details

The computational study of the key steps in the CBS-catalyzed reduction of acetophenone was carried out in vacuo by means of semiempirical calculations, as well as ab initio and DFT calculations.

The semiempirical calculations have been carried out using the AM1 model Hamiltonian<sup>51,52</sup> as implemented in AMSOL,<sup>53</sup> The source code was compiled for use on Silicon Graphics O<sup>2</sup> (Irix 6.5 operating system), Indigo<sup>2</sup> (Irix 5.3 operating system), and IBM RISC6000 workstations.

The ab initio calculations have been carried out at the Hartree–Fock (HF)<sup>54,55</sup> level, using the Gaussian 98 system of programs.<sup>56</sup> The

(36) Alagona, G.; Ghio, C.; Tomasi, S. *Theor. Chem. Acc.* (in press).

(37) Jones, D. K.; Liotta, D. C. *J. Org. Chem.* **1993**, *58*, 799–801.

(38) Linney, L. P.; Self, C. R.; Williams, I. H. *Tetrahedron: Asymmetry* **1994**, *5*, 813–816.

(39) Bringmann, G.; Hinrichs, J.; Kraus, J.; Wuzik, A.; Schulz, T. *J. Org. Chem.* **2000**, *66*, 2517–2527.

(40) Bach, J.; Berenguer, R.; Farrás, J.; Garcia, J.; Mesguer, J.; Villarasa, J. *Tetrahedron: Asymmetry* **1995**, *6*, 2683–2686.

(41) Puigjaner, C.; Vidal-Ferran, A.; Moyano, A.; Péricas, A. M.; Rieri, A. *J. Org. Chem.* **1999**, *64*, 7902–7911.

(42) Shen, Z.; Huang, W.; Feng, J.; Zhang, Y. *Tetrahedron: Asymmetry* **1998**, *9*, 1091–1095.

(43) Li, M.; Tian, A. *THEOCHEM* **2001**, *544*, 25–35.

(44) Li, M.; Xie, R.; Hu, C.; Wang, Z.; Tian, A. *Int. J. Quantum Chem.* **2000**, *78*, 245–251.

(45) Li, M.; Xie, R.; Tian, S.; Tian, A. *Int. J. Quantum Chem.* **2000**, *81*, 252–260.

(46) Li, M.; Zheng, X.; Hu, C.; Wang, Z.; Tian, A. *Int. J. Quantum Chem.* **2001**, *81*, 291–304.

(47) Reiners, I.; Martens, J.; Schwarz, S.; Henkel, H. *Tetrahedron: Asymmetry* **1996**, *7*, 1763–1770.

(48) Xingshu, L.; Rugang, X. *Tetrahedron: Asymmetry* **1996**, *7*, 2779–2782.

(49) Huang, H.-L.; Lin, Y.-C.; Chen, S.-F.; Wang, C.-L. J.; Liu, L. T. *Tetrahedron: Asymmetry* **1996**, *7*, 3067–3070.

(50) Trentmann, W.; Mehler, T.; Martens, J. *Tetrahedron: Asymmetry* **1997**, *8*, 2033–2043.

(51) (H, C, N, O) Dewar, M. J. S.; Zoebisch, E. G.; Healy, E. F.; Stewart, J. J. P. *J. Am. Chem. Soc.* **1985**, *107*, 3902–3909.

(52) (B) Dewar, M. J. S.; Jie, C.; Zoebisch, E. G. *Organometallics* **1988**, *7*, 513.

(53) Hawkins, G. D.; Giesen, D. J.; Lynch, G. C.; Chambers, C. C.; Rossi, I.; Storer, J. W.; Li, J.; Zhu, T.; Rinaldi, D.; Liotard, D. A.; Cramer, C. J.; Truhlar, D. G. *AMSOL*, version 6.5.3; Regents of the University of Minnesota: Minneapolis, MN, 1998.

(54) Pople, J. A.; Binkley, J. S.; Seeger, R. *Int. J. Quantum Chem.* **1976**, *10*, 1.

(55) Krishnan, R.; Frisch, M. J.; Pople, J. A. *J. Chem. Phys.* **1980**, *72*, 4244.

source code was compiled for use on a cluster of personal computers running under the Linux operating system and on DEC Alpha DS 20E Compaq workstations (Unix operating system).

Also in the density functional theory (DFT) framework, calculations have been carried out with Gaussian 98, using the B3LYP (Becke's three parameter hybrid functional using the LYP correlation functional)<sup>57</sup> and MPW1PW91 (Adamo and Barone's Becke-style one parameter functional using modified Perdew–Wang exchange and Perdew–Wang 91 correlation)<sup>58</sup> functionals.

Two split valence-shell basis sets have been employed: 3-21G<sup>59</sup> and 6-31G\*.<sup>60–63</sup>

The Kitaura and Morokuma decomposition of the interaction energy<sup>64</sup> was performed with GAMESS.<sup>65</sup>

The optimized AM1 structures were used as the starting point for the optimizations at the HF and DFT levels with the 3-21G basis set. The optimizations at the B3LYP/6-31G\* level used optimized HF/3-21G structures as input geometries when available, otherwise AM1 structures were employed.

TS search was carried out drawing a small section of the PES near the desired transition state. A grid was built with AM1, in which each point is an optimized structure with frozen carbonyl C-hydride (C••H) and carbonyl C-exocyclic B (C••B) coordinates. From inspection of the PES, two appropriate geometries on either side of the saddle point are selected and used to start the TS optimization with the SADDLE algorithm. The SADDLE algorithm makes use of the two input geometries to generate a guess of the transition state whose internal coordinates are the arithmetic mean of the two points selected and then minimizes the structure to the closest one with a single negative eigenvalue of the Hessian.

The AM1 transition state obtained in this way could be an acceptable guess for the ab initio transition state optimization. This method was tested for a case in which transition state energy and geometry were already known. Blake, Quallich, and Woodall calculated the transition state of the reduction of ketones with simpler oxazaborolidines than Corey's.<sup>35</sup> The TS search for the reaction of pinacolone (*tert*-butyl methyl ketone, *t*BMK) with their model oxazaborolidine–borane complex (compound 6 in the mentioned paper) yielded an HF/3-21G transition state identical to the one from the cited paper.

Vibrational frequencies were calculated for all the species at the HF/3-21G and B3LYP/6-31G\* levels. Transition state structures were confirmed as such by the existence of a single imaginary frequency.

Throughout this work,  $E$  will be used to denote potential energies at 0 K, without ZPE correction. Gibbs free energies,  $G$ , have been calculated adding ZPE, the thermal contributions and entropy at 298 K.

The parametrization of the AM1 Hamiltonian is such that the calculations yield heats of formation ( $\Delta H_f$ ). Therefore, AM1 transition states are obtained from enthalpy surfaces and not potential energy surfaces. It is assumed that the transition state obtained in this way is a good approximation of the TS on an ab initio (or DFT) potential energy surface.

## Results and Discussion

CBS reductions are particularly efficient with arylalkyl ketones, and acetophenone is historically the most used benchmark for evaluating the efficiency of new oxazaborolidines. Since the stereochemical outcome of the CBS reduction of acetophenone is already known, its study allows a computational model of the reaction to be developed and to be validated against experimental data.

According to Corey's catalytic cycle, the species involved in the key steps of the mechanism are the CBS catalyst, its complex with borane, the ketone–CBS–BH<sub>3</sub> adduct (with different geometries leading to different enantiomers), the transition states for the hydride transfer, and the transient oxazadiboretane intermediates. The crucial steps for stereo-selection are the complexation of acetophenone to CBS–BH<sub>3</sub> and the hydride transfer; thus a correct calculation of complex and TS geometries and energies is particularly important.

**Catalyst–Borane Complexation.** The energetic data obtained in this work for Corey's oxazaborolidine and its complex in which borane coordinates at nitrogen show that borane complexation is an exothermic reaction, leading to a stable complex. Indeed laboratory experience tells that CBS–BH<sub>3</sub> is a fairly stable compound that can be manipulated briefly even in the open air.

Although the geometries of the free oxazaborolidine calculated at the various levels of theory show rather different bond lengths and angles, they are qualitatively similar. In fact N, O, B, and the carbon linked to it lie in the same plane, while the N–O and B–O bonds are shorter than normal, all of which are evidence of a  $\pi$  system connecting the N, B, and O atoms.

As observed by Corey and co-workers,<sup>1</sup> borane coordination to the oxazaborolidine is spontaneous and rapid. To model the reaction more closely to that actually occurring in solution, the BH<sub>3</sub>•THF complex was used instead of free borane, differently from most of the papers dealing with this subject, so the data reported hereafter correspond to the in vacuo exchange reaction in which CBS substitutes THF as a ligand for borane. Energetic data from semiempirical (AM1), ab initio (HF/3-21G), and DFT (B3LYP/6-31G\*) calculations are consistent and indicate that the energy ( $\Delta E$ ) of the reaction between CBS and BH<sub>3</sub>•THF ranges from –4.42 to 18.55 kcal/mol, depending on the method adopted (AM1, HF/3-21G, B3LYP/6-31G\*) and on the geometry of the complex. When the contributions to the free energy are introduced, coordination at the HF/3-21G level is somewhat destabilized with respect to the internal energy calculations, from 4.06 to 5.58 kcal/mol for the cis mode and from 18.55 to 20.70 kcal/mol for the trans mode (cis and trans are indicating the spatial relationship between BH<sub>3</sub> and the hydrogen on C-4). A slightly favorable shift is observed when calculating free energies only at the B3LYP/6-31G\* level for the cis coordination free energy, which changes from –1.73 to –1.88 kcal/mol, whereas either the trans coordination or the other levels are less favorable, as shown in Table 2. While for both methods the trans coordination mode is unfavorable, for the cis coordina-

- (56) Frisch, M. J.; Trucks, G. W.; Schlegel, H. B.; Scuseria, G. E.; Robb, M. A.; Cheeseman, J. R.; Zakrzewski, V. G.; Montgomery, J. A.; Stratmann, R. E.; Burant, J. C.; Dapprich, S.; Millam, J. M.; Daniels, A. D.; Kudin, K. N.; Strain, M. C.; Farkas, O.; Tomasi, J.; Barone, V.; Cossi, M.; Cammi, R.; Mennucci, B.; Pomelli, C.; Adamo, C.; Clifford, S.; Ochterski, J.; Petersson, G. A.; Ayala, P. Y.; Cui, Q.; Morokuma, K.; Malick, D. K.; Rabuck, A. D.; Raghavachari, K.; Foresman, J. B.; Cioslowski, J.; Ortiz, J. V.; Stefanov, B. B.; Liu, G.; Liashenko, A.; Piskorz, P.; Komaromi, I.; Gomperts, R.; Martin, R. L.; Fox, D. J.; Keith, T.; Al-Laham, M. A.; Peng, C. Y.; Nanayakkara, A.; Gonzalez, C.; Challacombe, M.; Gill, P. M. W.; Johnson, B. G.; Chen, W.; Wong, M. W.; Andres, J. L.; Head-Gordon, M.; Replogle, E. S.; Pople, J. A. *Gaussian 98*, revision A.6; Gaussian, Inc.: Pittsburgh, PA, 1998.
- (57) (a) Becke, A. D. *J. Chem. Phys.* **1993**, *98*, 5648. (b) Lee, C.; Yang, W.; Parr, R. G. *Phys. Rev. B* **1988**, *37*, 785.
- (58) Adamo, C.; Barone, V. *J. Chem. Phys.* **1998**, *108*, 664.
- (59) Binkley, J. S.; Pople, J. A.; Hehre, W. J. *J. Am. Chem. Soc.* **1980**, *102*, 939.
- (60) Ditchfield, R.; Hehre, W. J.; Pople, J. A. *J. Chem. Phys.* **1971**, *54*, 724.
- (61) Hehre, W. J.; Ditchfield, R.; Pople, J. A. *J. Chem. Phys.* **1972**, *56*, 2257.
- (62) Dill, J. D.; Pople, J. A. *J. Chem. Phys.* **1975**, *62*, 2921.
- (63) Hariharan, P. C.; Pople, J. A. *Theor. Chim. Acta* **1973**, *28*, 213.
- (64) Kitaura, K.; Morokuma, K. *Int. J. Quantum Chem.* **1976**, *10*, 325.
- (65) Schmidt, M. W.; Baldridge, K. K.; Boatz, J. A.; Elbert, S. T.; Gordon, M. S.; Jensen, J. H.; Koseki, S.; Matsunaga, M.; Nguyen, K. A.; Su, S. J.; Windus, T. L.; Dupuis, M.; Montgomery, J. A. *J. Comput. Chem.* **1993**, *14*, 1347–1363.

**Table 2.** Reaction Energetics for the Coordination of Borane to Corey's Oxazaborolidine, Computed at the B3LYP/6-31G\*, HF/3-21G, and AM1 Levels<sup>a</sup>

	AM1 <sup>a</sup>		HF/3-21G		B3LYP/6-31G*	
	$\Delta H_i$	$\Delta H$	$E^b$	$\Delta E^b$	$E^b$	$\Delta E^b$
BH <sub>3</sub>	26.26		-26.237 302		-26.613 000	
THF	-58.40		-229.699 158		-232.449 443	
BH <sub>3</sub> •THF	-47.65		-255.981 580		-259.096 303	
CBS	-21.15		-842.685 294		-852.879 062	
CBS–BH <sub>3</sub> , cis	-14.82	-4.42	-868.961 238	4.06	-879.528 683	-1.73
CBS–BH <sub>3</sub> , trans <sup>c</sup>	na <sup>d</sup>	na <sup>d</sup>	-868.938 148	18.55	-879.513 299	7.92

	AM1 <sup>a</sup>		HF/3-21G		B3LYP/6-31G*	
	$\Delta G_i$	$\Delta G$	$G^b$	$\Delta G^b$	$G^b$	$\Delta G^b$
BH <sub>3</sub>	33.28		-26.227 942		-26.604 058	
THF	-2.57		-229.601 619		-232.360 791	
BH <sub>3</sub> •THF	29.83		-255.852 778		-258.976 448	
CBS	170.04		-842.359 631		-852.580 141	
CBS–BH <sub>3</sub> , cis	198.95	-3.49	-868.601 892	5.58	-879.198 781	-1.88
CBS–BH <sub>3</sub> , trans <sup>c</sup>	na <sup>d</sup>	na <sup>d</sup>	-868.577 801	20.70	-879.179 995	9.92

<sup>a</sup> In kcal/mol. <sup>b</sup> Absolute energies and free energies in Hartree. <sup>c</sup> cis and trans are indicating the spatial relationship between BH<sub>3</sub> and the hydrogen on C-4; see Figure 1. <sup>d</sup> Not available. <sup>e</sup> Coordination energies and free energies, referring to BH<sub>3</sub>•THF and CBS at infinite distance, are reported.

tion mode, the HF and DFT results are not in agreement. B3LYP/6-31G\* (and AM1) results agree in describing the process as favorable, whereas at the HF/3-21G level the exchange reaction between CBS and BH<sub>3</sub>•THF is unfavorable, due to a high BSSE<sup>36</sup> and to the well-known HF/3-21G overestimate of electrostatic interactions, artificially stabilizing BH<sub>3</sub>•THF. Calculations using free borane (reported later in Figure 7) yielded more favorable coordination energies and free energies, respectively, by 21.25 and 7.28 kcal/mol with B3LYP/6-31G\*, by 15.51 and 0.88 kcal/mol with AM1, and finally by 28.31 and 14.57 kcal/mol with HF/3-21G.

Although more accurate results would require an explicit treatment of solvent effects, the obtained energy values are substantially in agreement with Corey's statement that the initial step is probably reversible. Nevertheless, nothing can be said about the coordination rate, since nothing about its activation energy is known. The results are consistent also with those by Quallich, Blake, and Woodall, who, for their nonfused ring systems, closer to Itsuno's than to Corey's, report that the cis complexation of BH<sub>3</sub> is favored over the trans one.<sup>35</sup> Due to

the presence of the proline ring, conferring rigidity to the system, in the case of the full CBS system, this difference is even more evident.

The coordination of borane to CBS has important effects on the electronic structure of the catalyst, which is responsible for its high activity. Its consequence is that the electron density shifted from the nitrogen to the boron enhances the nucleophilicity of the hydrides and the Lewis acid characteristic of the endocyclic boron. In the cis CBS–BH<sub>3</sub> complex, the N atom donates to BH<sub>3</sub> its lone pair, which for this reason is no longer available for delocalization in the  $\pi$  system. In fact, the lone pair of nitrogen on the free oxazaborolidine is delocalized in a  $\pi$  system giving the N–B bond a partial double bond character that is lost after complexation of borane. This change is reflected by the B–N bond distances, which increase from 1.410 Å in the free oxazaborolidine to 1.498 Å after complexation with BH<sub>3</sub>. Similar values are reported in the works of Nevalainen<sup>13</sup> and Quallich, Blake, and Woodall.<sup>35</sup> At the highest level of theory used (B3LYP/6-31G\*), the optimized CBS–BH<sub>3</sub> geometry is very close to that obtained from X-ray diffraction measurements, proving that the structure prediction is good at the B3LYP/6-31G\* level of theory and acceptable even at the HF/3-21G level (see Figure 2 and Table 3). Furthermore, all calculations performed with the HF and DFT methods correctly describe the ring puckering, in contrast to the AM1 Hamiltonian, which describes the oxazaborolidine ring as planar. The orientation of the upper phenyl substituent, as described by all the methods used, is slightly rotated as compared with the structure of crystalline CBS–BH<sub>3</sub>.

A key factor for the performance of Corey's catalyst is its enhanced rigidity, a consequence of the presence of the fused proline ring. In the case of Corey's catalyst, the coordination of the BH<sub>3</sub> moiety trans with respect to the hydrogen on C-4 forces the proline ring to assume a high-energy twisted conformation. Indeed, this is what is found from the HF/3-21G and B3LYP/6-31G\* levels: the trans complexation mode is destabilized, compared with the cis one, by 10–15 kcal/mol, depending on the level (see Table 2). Additionally, in the trans complex, the N–B<sub>exocyclic</sub> separation is considerably longer (0.03 Å with HF/3-21G) than in the cis complex, as pointed out also by Nevalainen for a reduced model of the CBS–BH<sub>3</sub> complex.<sup>13</sup> In more flexible systems, like those studied by Quallich, Blake, and Woodall, the preference for this geometry is less strong but still existing, because the unfavorable steric interaction with

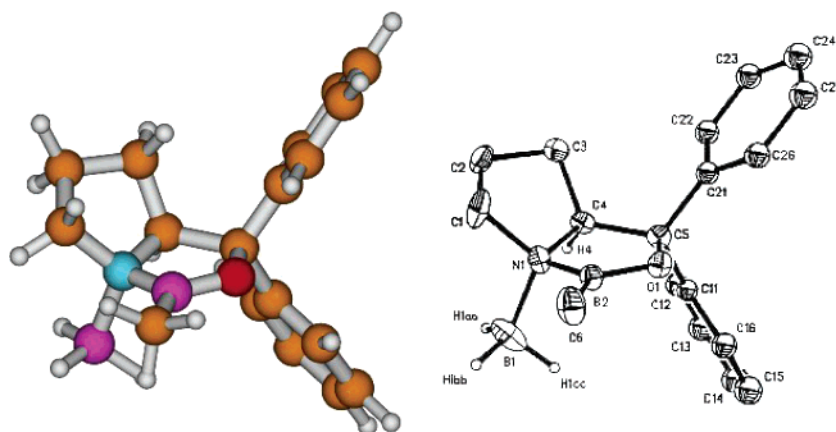


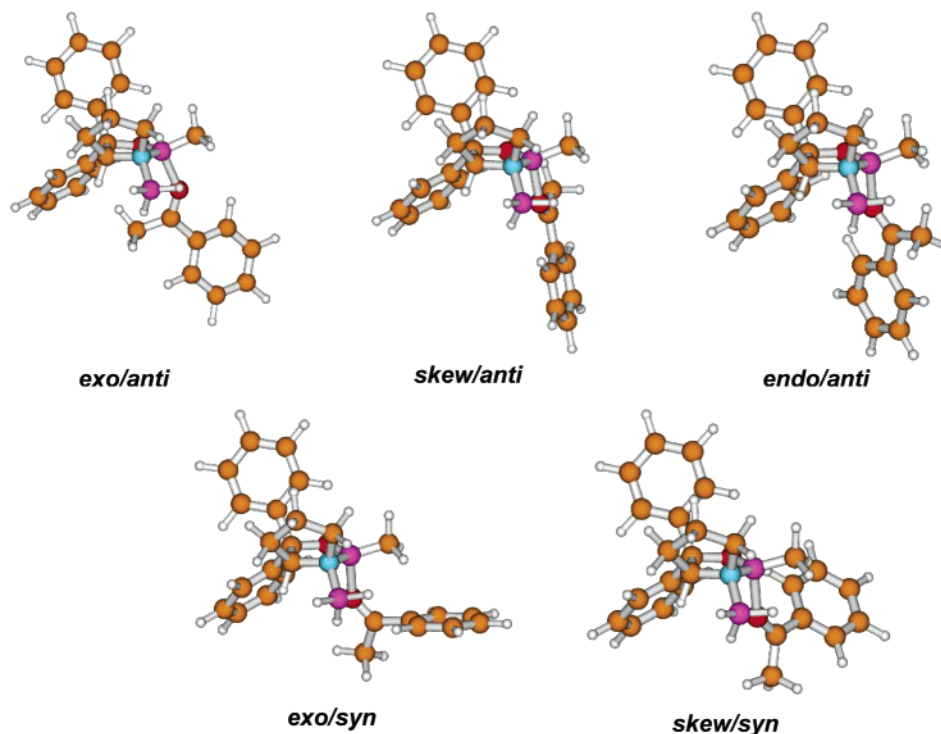
**Figure 2.** B3LYP/6-31G\* and observed (ref 9) geometries of the CBS–BH<sub>3</sub> complex (BH<sub>3</sub> and H on C-4 are in a cis relationship).



**Table 3.** Selected Computed and Observed Interatomic Distances of the *cis* CBS–BH<sub>3</sub> Complex (Expressed in Å)

source calculation level	this work				observed (ref 9)	ref 35 <sup>a</sup>		ref 13 <sup>b</sup>
	AM1	HF/3-21G	HF/6-31G*	B3LYP/6-31G*		HF/3-21G	HF/6-31G*	HF/6-31G
N–B <sub>exocyclic</sub>	1.631	1.709	1.705	1.680	1.62	1.729	1.712	1.713
N–B <sub>endocyclic</sub>	1.510	1.507	1.490	1.498	1.486	1.512	1.495	1.496
O–B <sub>endocyclic</sub>	1.369	1.378	1.343	1.357	1.335	1.378	1.346	1.356

<sup>a</sup> Borane adduct of compound **6** in Figure 1 of ref 35. <sup>b</sup> Compound **2'd** in Table 2 of ref 13.

**Figure 3.** *exo/anti*, *exo/syn*, *endo/anti*, *skew/anti*, and *skew/syn* conformations of acetophenone complexes with CBS–BH<sub>3</sub> computed at the AM1 level.

the substituent on C-4 destabilizes the coordination of BH<sub>3</sub> from the upper face of the oxazaborolidine. Furthermore, the N–B<sub>exocyclic</sub>, N–B<sub>endocyclic</sub>, and O–B<sub>endocyclic</sub> separations in their systems at the HF/3-21G and HF/6-31G\* levels are quite similar to those calculated in this work, irrespective of the substitution pattern around the oxazaborolidine core.<sup>36</sup>

**CBS–BH<sub>3</sub>–Acetophenone Complexes.** The groups on the chiral catalyst force the ketone approach from the less hindered face of the oxazaborolidine, which in the usual representation (shown in Figure 2) is the lower side. The empty region through which the ketone can draw near has a roughly conic shape; inside this ideal cone, the ketone can assume different orientations relative to the oxazaborolidine, giving rise to complexes of distinct conformations. Classification of the different complexes is important because the stereochemical outcome of the reduction depends on the conformation of the BH<sub>3</sub>–CBS–ketone complex.

According to the nomenclature used by García, Farras, and co-workers,<sup>40</sup> the complex will be called *exo* or *endo* depending on the absolute value of the C–B••O=C dihedral angle formed by the C atom attached to the endocyclic B atom, the B atom itself and the carbonyl O and C atoms. If it is close to 180°, the geometry will be *endo*; if it is close to 60°, it will be *exo*.

Similarly, the value of the B••O=C–R<sub>L</sub> dihedral angle determines whether the complex is either *syn* or *anti*, R<sub>L</sub> indicating the ketone side group with the higher priority

according to the Cahn–Ingold–Prelog priority rules. If the absolute value of the dihedral angle is close to 0°, the geometry is *syn*, while if it is close to 180°, it is *anti*. The two torsions are not defined when the BOC angle is 180°, and the distinction between the complexation modes is more significant as the value of this angle decreases.

Out of the four complexes that we can imagine for acetophenone, the *exo/syn* and *endo/anti* complexes offer the **Re** face for hydride attack. In the *exo/anti* and *endo/syn* complexes of acetophenone, the exposed face is the **Si** face, which leads to the product that is preferentially formed in the experiment. So at least one transition state stemming from these two complexes must be the one determining the outcome of the reaction.

If, as stated by Corey,<sup>1</sup> both the ketone complexation and the highly exothermic hydride transfer are probably fast and comparably rate-limiting, then by the Hammond postulate<sup>66</sup> complexes and transition states will have similar geometries and probably be ordered with the same relative stability. If this were true, it would be sufficient to compute the relative stability of the complexes to predict qualitatively the chirality of the product.

As a common procedure, adopted also in the following parts of this work, the catalyst–ketone complexes have been optimized first with the faster AM1 semiempirical method.

Input geometries roughly corresponding to the complexes in the four conformations were optimized, but only three of them resulted to be local minima (see Figure 3). No local minimum



**Table 4.** Geometric Data of the Stable Conformations of Acetophenone Complexes with CBS–BH<sub>3</sub>, Computed at the B3LYP/6-31G\*, B3LYP/3-21G, MPW1PW91/3-21G, HF/3-21G, and AM1 Levels of Theory<sup>a</sup>

	CBOC	BOCPh	BOC	C–O	O–B <sub>endo</sub>	B <sub>exo</sub> –N	N–B <sub>endo</sub>	B <sub>exo</sub> –H	H–C
B3LYP/6-31G*									
exo/anti	36.9	178.2	139.1	1.250	1.712	1.641	1.567	1.216	2.787
skew/anti	–75.5	176.0	133.0	1.248	1.669	1.654	1.565	1.217	3.656
B3LYP/3-21G									
exo/anti	41.7	175.4	139.3	1.244	1.660	1.661	1.574	1.216	2.771
exo/syn	–13.0	48.8	147.2	1.265	1.739	1.650	1.569	1.216	3.211
skew/anti	–77.2	175.0	132.9	1.272	1.652	1.666	1.572	1.216	3.670
MPW1PW91/3-21G									
exo/anti	46.1	171.5	137.9	1.268	1.625	1.630	1.579	1.224	2.546
exo/syn	–10.3	41.5	145.0	1.262	1.678	1.631	1.565	1.219	3.173
skew/anti	–80.6	174.4	132.7	1.268	1.626	1.647	1.566	1.221	3.644
HF/3-21G									
exo/anti	41.7	175.4	143.6	1.244	1.660	1.661	1.574	1.216	2.717
skew/syn	–42.5	–27.2	151.5	1.239	1.681	1.679	1.560	1.214	3.425
skew/anti	–75.4	173.6	135.8	1.244	1.651	1.676	1.564	1.214	3.687
AM1									
exo/anti	54.9	178.4	132.7	1.258	1.822	1.606	1.554	1.211	2.481
exo/syn	26.5	–1.4	136.9	1.246	1.877	1.608	1.551	1.210	2.676
endo/anti	–179.0	–179.6	141.9	1.252	1.861	1.613	1.548	1.210	2.565
skew/syn	–34.8	–14.1	129.7	1.245	1.897	1.620	1.547	1.209	3.210
skew/anti	–69.8	177.0	140.4	1.256	1.815	1.620	1.552	1.211	3.368

<sup>a</sup> Interatomic distances are in Å, and angles, in deg. B<sub>exo</sub>–H and H–C indicate the interatomic distances involving the hydride closest to the carbonyl group.

corresponding to the endo/syn conformation was actually found. Instead, a different, new conformation was found, in which the C–B••O=C dihedral angle measured approximately –70° and the B••O=C–R<sub>L</sub> one, about 177°, as shown in Table 4.

As a consequence of this finding, in addition to the expected complexes, a new type was defined, named skew, because of the value of the C–B••O=C dihedral (close to –60°). The skew/anti conformation is less stable (~1.4 kcal/mol) than the exo/anti one, while it is somewhat more stable than both the exo/syn and endo/anti ones by 1.3 and 0.7 kcal/mol, respectively (see Table 5). Following the location of the skew/anti conformation, another local minimum was found, corresponding to a skew/syn arrangement. Among the optimized complexes, this is the least stable (~4.5 kcal/mol above exo/anti).

Although the existence of skew conformations was unexpected, failure to locate them would not have been really misleading, because they probably do not play a direct role in the reduction. In fact, as can be seen from Figure 3, the carbonyl group points away from the hydride in skew complexes. In the skew/anti complex, the AM1 distance between C and H atoms is 3.4 Å (3.7 Å at the HF/3-21G and B3LYP/6-31G\* levels), and in both skew complexes, the hydride lies almost exactly on the nodal plane of the carbonyl group. For the intramolecular delivery of a hydride to occur, acetophenone first would have to rotate about the B••O “bond” or invert the B••O=C angle, assuming in that way one of the reactive conformations, or dissociate and eventually form a new complex of a suitable conformation.

Wiberg and LePage calculated the barrier for the rotation about the B••O “bond” and for the inversion of the B••O=C angle in the complex between BH<sub>3</sub> and H<sub>2</sub>C=O. At the HF/3-21G level of theory, they obtained values of 1.25 and 7.66 kcal/mol, respectively, which are substantially lower than the

**Table 5:** Reaction Energetics for the Reduction of Acetophenone with the CBS–BH<sub>3</sub> Complex, Computed at the B3LYP/6-31G\*, HF/3-21G, and AM1 Levels<sup>a</sup>

	ΔE (compl)	E <sub>rel</sub> (TS)	ΔE (reaction)	ΔG (compl)	G <sub>rel</sub> (TS)	ΔG (reaction)
B3LYP/6-31G* <sup>a</sup>						
exo/anti	2.19	4.86	–32.36 <sup>e</sup>	19.04	22.51	–13.41 <sup>e</sup>
exo/syn	<i>d</i>	8.99	–31.43 <sup>f</sup>		25.76	–12.52 <sup>f</sup>
endo/anti	<i>d</i>	8.97	–31.43 <sup>f</sup>		26.81	–12.52 <sup>f</sup>
skew/anti	1.97			18.34		
HF/3-21G <sup>b</sup>						
exo/anti	–8.70	–1.97	–61.40 <sup>e</sup>	8.39	15.57	–41.32 <sup>e</sup>
exo/syn	<i>d</i>	2.03	–61.50 <sup>f</sup>		18.71	–42.15 <sup>f</sup>
endo/anti	<i>d</i>	1.49	–61.50 <sup>f</sup>		18.88	–42.15 <sup>f</sup>
skew/syn	–4.27			11.39		
skew/anti	–8.04			8.20		
	ΔH (compl)	ΔH <sub>f</sub> (TS) <sub>rel</sub>	ΔH (reaction)	ΔG (compl)	G <sub>rel</sub> (TS)	ΔG (reaction)
AM1 <sup>c</sup>						
exo/anti	–0.76	3.75	–38.06 <sup>e</sup>	17.70	19.80	–20.70 <sup>e</sup>
exo/syn	1.92	5.76	–40.49 <sup>f</sup>	17.80	22.27	–23.05 <sup>f</sup>
endo/anti	1.32	6.09	–40.49 <sup>f</sup>	18.68	23.04	–23.05 <sup>f</sup>
skew/syn	3.72			18.19		
skew/anti	0.62			16.39		

<sup>a</sup> Reference energies are  $E = -1264.424\ 674$  au and  $G = -1263.989\ 033$  au. <sup>b</sup> Reference energies are  $E = -1249.301\ 775$  au and  $G = -1248.825\ 049$  au. <sup>c</sup> Reference energies are  $\Delta H_f = -29.83$  kcal/mol and  $G = 251.307$  kcal/mol. <sup>d</sup> The skew/anti conformation was obtained instead. <sup>e</sup> Product having (R) chirality. <sup>f</sup> Product having (S) chirality. <sup>g</sup> Energies and free energies in kcal/mol, referring to acetophenone and CBS–BH<sub>3</sub> at infinite distance.

calculated coordination energy of 17.1 kcal/mol.<sup>67</sup> It is likely that the coordination energy and barrier heights to rotation and inversion can be influenced by the sterical demand of substituent groups, thus suggesting that these values may not be extended acritically to our case.

To check the reliability of the picture obtained that can heavily depend on the strategy employed, that is, the optimization of rough structures built in the vicinity of the expected conformations, a thorough examination of the potential energy surface (PES) of the conformers was performed at the AM1 level. A large number of ketone–catalyst complexes, each with a different couple of fixed values for the two dihedrals, were optimized until the complete surface was mapped. After cubic interpolation between the data points, the PES was drawn (Figure 4).

In some regions of the map, the B••O=C angle tended to assume a value of 180° during the optimizations. Under these conditions the C–B••O=C and B••O=C–R<sub>L</sub> dihedrals are undefined; therefore, the optimizations could not successfully be carried out. Because of this reason, not all the points of the grid could be calculated, so the quality of the interpolated surface in the areas with lower density of grid points is poorer. However, this problem was encountered only in high energy regions, while in the most important parts the quality of the surface is good enough to confirm its relevant features, that is, that, according to AM1, all conformations except the endo/syn one correspond to local minima, and namely the skew complexes exist and the skew/anti one is rather stable.

The high energy of endo conformations is generally explained in terms of the repulsion between the R<sub>L</sub> group of acetophenone, that is, the phenyl substituent, and the phenyl group on the lower

(66) Hammond, G. S. *J. Am. Chem. Soc.* **1955**, *77*, 334–338.(67) Wiberg, K.; LePage, T. *J. Am. Chem. Soc.* **1988**, *110*, 6642–6650.

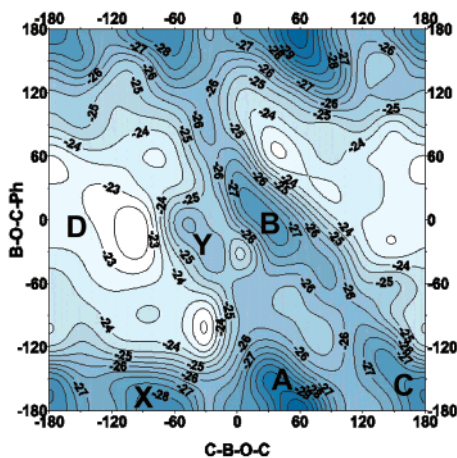


**Figure 4.** AM1 potential energy surface (in kcal/mol) of the conformers of CBS-acetophenone, for the rotation about CBOC and BOCP (in deg). A, B, C, D, X, and Y indicate the exo/anti, exo/syn, endo/anti, endo/syn, skew/anti, and skew/syn conformations, respectively. The endo/syn conformation does not correspond to a stable complex since it is located in a high-energy region.

face of the oxazaborolidine,<sup>25</sup> and this is particularly true for the endo/syn complex. The vast amount of experiments shows clearly the superiority of 5,5'-disubstituted oxazaborolidines over 5-monosubstituted ones, having the phenyl substituent only on the upper face, but the importance of this group has not been rationalized thus far, since up to now a reliable high-level computational study of all the possible complex conformations was lacking.

As already mentioned, the geometries obtained with AM1 were used as starting points for further ab initio optimizations. The initial trial employing a relatively simple combination of methods with the smallest split valence shell basis set, that is, HF/3-21G, produced unpredictable results. As in the semi-empirical calculations, the exo/anti conformation appeared to be lower in energy than the skew complexes; the optimization starting from an endo/syn conformation produced again the skew/anti complex. In contrast to AM1 calculations, and unexpectedly, exo/syn and endo/anti conformations were not local minima at the HF/3-21G level, and they too evolved to the skew/anti geometry. The only stable complexes found at the B3LYP/6-31G\* level are the exo/anti and skew/anti ones. According to the modeling studies reported elsewhere,<sup>36</sup> this has been considered the most reliable among the levels used.

From a perusal of Table 5, several remarkable differences emerge in the description given on one side by the AM1 method and on the other one by the HF and DFT methods. The most evident difference is the number of stable complex conformations at the AM1 level (five), as opposed to just two stable complexes found at the B3LYP/6-31G\* level.

Other noticeable differences are the amplitude of the B··O separation (see Table 4), which according to the calculations carried out at the AM1 level is over 0.1 Å wider than that obtained at the HF and DFT levels, and the stability order among the complexes. Free energy calculations (also reported in Table 5) show that the reactant complexes are sharply destabilized at all levels, thus producing a sensitive increase in the free energy reaction profiles with respect to the potential energy ones. The exo/anti and the skew/anti conformations are almost isoenergetic at the HF/3-21G and B3LYP/6-31G\* levels, whereas with AM1 the skew/anti structure is more stable by 1.31 kcal/mol than

**Table 6.** 3-21G Complexation Energy (kcal/mol) of Acetophenone with CBS-BH<sub>3</sub>, Computed at the B3LYP, MPW1PW91, and HF Levels, Referring to Acetophenone and CBS-BH<sub>3</sub> at Infinite Separation

	3-21G	HF <sup>a</sup>	B3LYP <sup>b</sup>	MPW1PW91 <sup>c</sup>
exo/anti		-8.70	-11.72	-15.51
exo/syn		<i>d</i>	-6.02	-9.33
skew/anti		-8.04	-11.04	-14.43

<sup>a</sup> Reference energy  $E = -1249.301\,775$  au. <sup>b</sup> Reference energy  $E = -1257.523\,028$  au. <sup>c</sup> Reference energy  $E = -1257.216\,219$  au. <sup>d</sup> The skew/anti conformation was obtained instead.

the exo/anti one. Interestingly enough, the AM1 values are generally closer to the B3LYP/6-31G\* ones than the HF/3-21G ones. However, the shape of the ab initio or DFT potential energy surface could probably be quite different from the AM1 PES (Figure 4). For these reasons, results from AM1 calculations must always be taken with great caution and, if possible, compared with data from higher level (HF or DFT) calculations.

No local minima, of any conformation, were detected at the HF/6-31G\* level of theory. In this case, the factors artificially stabilizing the complexes at the HF/3-21G level, that is, strong electrostatic interactions and high BSSE, are reduced, while electron correlation effects are still neglected.

Conversely, DFT calculations (B3LYP, MPW1PW91) with the smaller basis set (3-21G), reported in Table 6, describe the exo/syn conformation as stable but fail with the endo/anti one.

**Hydride Transfer Transition States and Intermediate Products.** The transition state search starts from the substrate-catalyst complexes.

There are no general methods for locating a first-order transition state whose success is guaranteed.<sup>68</sup> In a complex system like that under scrutiny, the most simple method, consisting in iteratively converging the molecular geometry to the closest point in which the first derivatives of potential energy vanish (which corresponds to a stationary point), while one eigenvalue of the Hessian matrix has a negative sign (which indicates that the stationary point is a first order saddle point), will most likely end finding a conformational TS whose geometry is much closer to the "reactant" than to the desired hydride transfer TS. Therefore, the only way to have a greater chance of success is to use a better guess for the transition state, that is, a structure closer to it. This requires the determination of the leading parameters of the reaction.

The hydride and the carbonyl carbon in the complex are too far away for the internal hydride delivery to occur, so the complex must distort its geometry from that of the local minimum, to allow H and C to reach a proper distance, without raising its energy too much. The reaction coordinate is therefore described by the C··H and the C··B distances, which have been selected to conveniently draw a small section of the PES near the desired transition state. As with the conformational map of the acetophenone-CBS complexes, it is necessary first to build a grid, in which each point is an optimized structure with frozen C··H and C··B coordinates. Finally, from a PES inspection, the appropriate geometries are selected and used to start the TS search.

(68) McKee, M. L.; Page, M. Computing Reaction Pathways on Molecular Energy Surfaces. In *Reviews in Computational Chemistry*; Lipkowitz, K. B., Boyd, D. B., Eds.; VCH Publishers Inc.: New York, 1993; Vol. IV, pp 35-65.

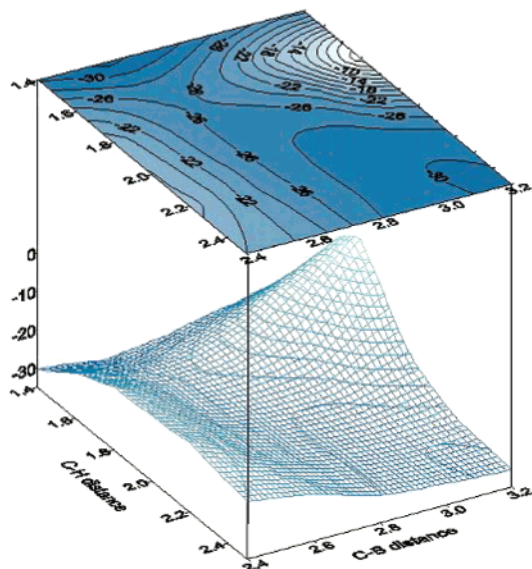


**Figure 5.** AM1 potential energy surface for the reduction of acetophenone with Corey's oxazaborolidine. Distances are in Å, and energies, in kcal/mol.

The weak point of this approach is that a great number of calculations is involved, and it would be practically unviable using ab initio methods. However, AM1 semiempirical calculations are fast enough to calculate the necessary grid points in a reasonable time. The AM1 transition state obtained after optimization of an appropriately chosen geometry could be an acceptable guess for the ab initio transition state optimization.

This transition state search method has been applied to the exo/anti acetophenone–MeCBS–BH<sub>3</sub> complex, giving the PES shown in Figure 5. The AM1 geometry of the transition state, determined as explained above, was then used for the HF/3-21G optimization.

The comparison of the interatomic distances of the six-membered ring that characterize the transition state for the acetophenone reduction with those reported in ref 35 reveals that the geometries are very close to each other even if the systems bear quite different side groups. Therefore, it is reasonable to assume that the hydride transfer in the acetophenone TS's having different conformations could approximately occur at the same C··H and C··B distances and that the shape of the PES should be similar.

On this basis, it is no longer necessary to build all the PES, but it is sufficient to perform a smaller number of calculations, each of them roughly corresponding to a point in the bottom of the valley that ends up with the saddle point.

This abbreviated method has been successfully applied to the search of the AM1 transition states of the endo/anti and exo/syn conformations, while the geometries obtained were used as inputs for the optimizations at the HF/3-21G level (Tables 5 and 7). The HF/3-21G transition states have been characterized by analyzing their vibrational modes, which showed an imaginary frequency, corresponding to the stretching of the B–H bond pointing toward the carbonyl. The complex and TS geometries obtained at the HF/3-21G level have been used as starting points for B3LYP/6-31G\* optimizations (Figure 6) and subsequent vibrational analyses, whose results are reported in Tables 5 and 7.

**Table 7.** Geometric Data for the TS's of Acetophenone Reduction with CBS–BH<sub>3</sub>, Computed at the B3LYP/6-31G\*, HF/3-21G, and AM1 Levels of Theory<sup>a</sup>

	CBOC	BOCPh	C–O	O–B <sub>endo</sub>	B <sub>exo</sub> –N	N–B <sub>endo</sub>	B <sub>exo</sub> –H	H–C
B3LYP/6-31G*								
exo/anti	71.7	151.1	1.288	1.566	1.585	1.618	1.278	1.679
exo/syn	72.7	–60.9	1.260	1.668	1.612	1.588	1.240	2.001
endo/anti	165.5	–148.8	1.279	1.574	1.604	1.623	1.262	1.764
HF/3-21G								
exo/anti	72.4	146.2	1.287	1.571	1.611	1.612	1.277	1.679
exo/syn	80.0	–72.7	1.274	1.602	1.618	1.603	1.255	1.767
endo/anti	165.1	–145.8	1.289	1.557	1.620	1.629	1.270	1.667
AM1								
exo/anti	79.7	152.8	1.301	1.666	1.595	1.572	1.262	1.667
exo/syn	78.8	–56.7	1.283	1.746	1.580	1.582	1.249	1.724
endo/anti	163.3	–143.0	1.295	1.682	1.584	1.587	1.251	1.700

<sup>a</sup> Interatomic distances are in Å, and angles, in deg. B<sub>exo</sub>–H and C–H indicate the interatomic distances involving the hydride closest to the carbonyl group.

According to the computational results, the reaction should proceed preferentially through the exo/anti transition state, giving a product of the same chirality as that obtained experimentally.

From an inspection of TS geometries, exo TS's appear to have a chairlike conformation, whereas the endo/anti TS has a boatlike conformation, as Blake, Quallich, and Woodall already observed from the examination of their models.<sup>35</sup> Also Jones and Liotta, in their MNDO study of the acetophenone reduction with CBS–BH<sub>3</sub>, found exo transition states with a chairlike conformation.<sup>37</sup> Other authors, like Williams and co-workers, Bringmann and co-workers, and Péricas and co-workers,<sup>17,39,41</sup> found TS's with either boatlike or chairlike conformations, depending on the oxazaborolidine–ketone complexation manner. In all cases, it was found that chairlike TS's were generated from exo complexes, whereas endo complexes led to boatlike TS's. Furthermore, chairlike TS's resulted to be lower in energy.

For the exo/syn TS at the B3LYP/6-31G\* level, a longer than normal C–H distance was found. This is a peculiar result, since in general in the literature bond distances in the six-membered cyclic TS do not vary much depending on the systems being studied or the levels of theory that are applied. However, from the analysis of the normal vibrational mode associated to the transformation from reactant to product, it was seen that the nuclear motions are very similar to those of the other TSs, that is, a motion of the hydride toward the carbonyl C and simultaneous rotation of the BH<sub>3</sub> group. This last motion is necessary if the hydride is to come as close as possible to the carbonyl C and is more pronounced in the B3LYP/6-31G\* exo/syn TS. This fact and the C–H distance, longer than normal, are hints of an earlier TS, compared to those obtained from other geometries and methods.

The oxazadiboretane structure presented by Corey and observed in NMR studies at very low temperature<sup>20</sup> was found from calculations too,<sup>15–19</sup> and it is much lower in energy than the reactants, showing that the hydride transfer step is very favorable and exothermic. This provides the thermodynamic drive responsible for the excellent yields obtained with this kind of reductions, as shown also in the energy profiles reported in Figure 7.

Following the lowest energy path on the PES, that is, using couples of values for the leading parameters along the bottom of the valley, beyond the transition state, the stable reduced



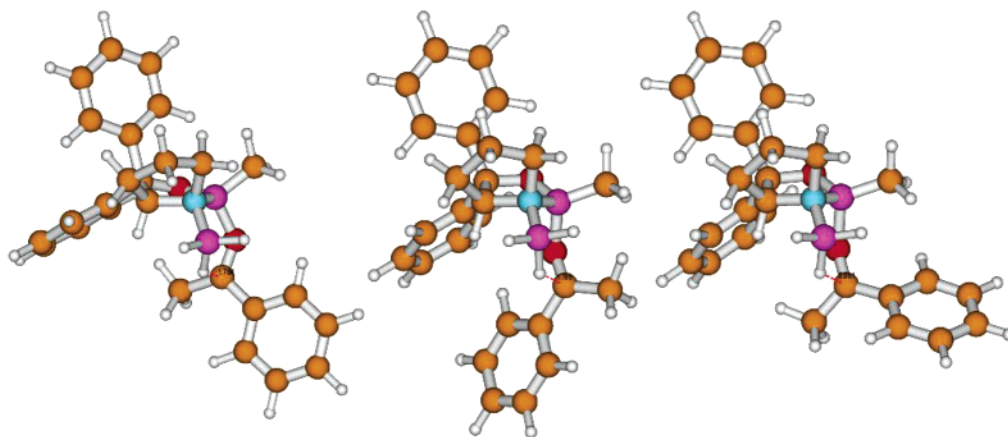


**Figure 6.** Transition state geometries for the reduction of acetophenone with Corey's oxazaborolidine in the endo/anti, exo/anti, and exo/syn geometries (optimized at the B3LYP/6-31G\* level).

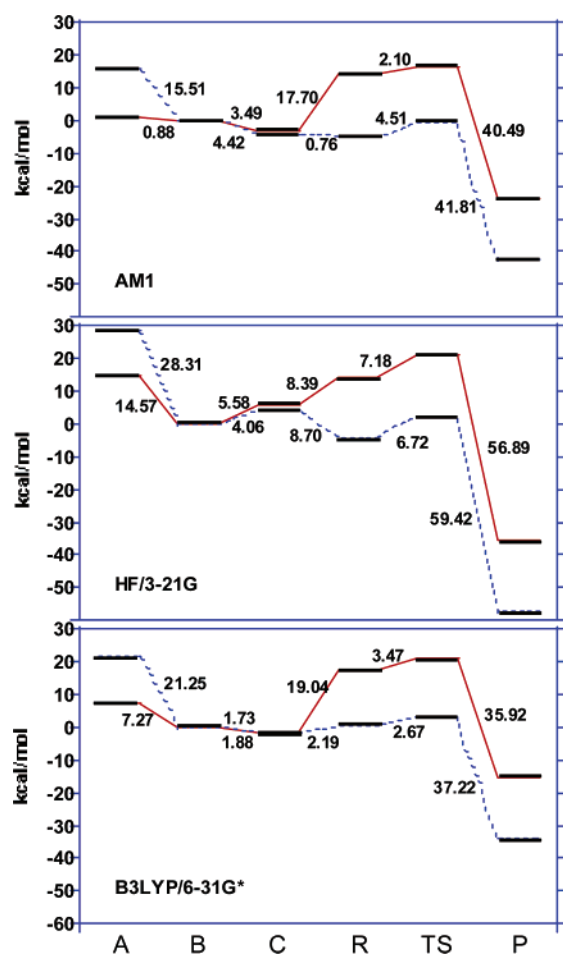


**Figure 7.** AM1 (top), HF (middle), and B3LYP (bottom) reaction profiles for the exo/anti pathway: relative enthalpies or energies (dashed lines) and free energies (solid lines). The gaps between the various levels are also shown. A = CBS, PhMK, THF, and BH<sub>3</sub> at infinite distance; B = CBS, BH<sub>3</sub>•THF, and PhMK at infinite distance; C = CBS–BH<sub>3</sub>, PhMK, and THF at infinite distance; R = reacting complex; TS = transition state; P = oxazadiboretane intermediate product.

intermediate at the AM1 level was reached. Geometries at the HF/3-21G and B3LYP/6-31G\* levels of theory were obtained as described above (see Figure 8 and Tables 5 and 8).

From the analysis of the B3LYP/6-31G\* results, it appears not only that the complexation is more endothermic than at the HF/3-21G and AM1 levels but also that the reaction is

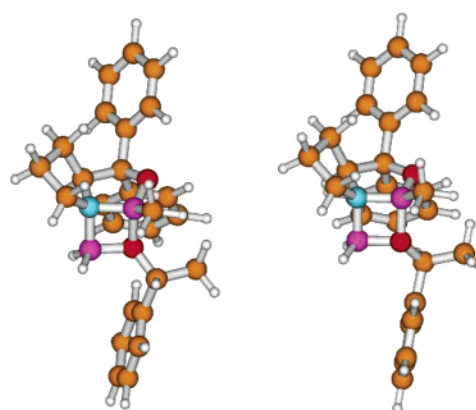


**Figure 8.** Products from the reduction of exo/anti, exo/syn, and endo/anti conformations computed at the B3LYP/6-31G\* level. The exo/anti geometry leads to the (R) configuration product (left), while the others to the (S) configuration product (right).

**Table 8.** Geometric Data for the Product of Acetophenone Reduction with CBS–BH<sub>3</sub>, Computed at the B3LYP/6-31G\*, HF/3-21G, and AM1 Levels of Theory<sup>a</sup>

	CBOC	BOCPh	C–O	O–B <sub>endo</sub>	B <sub>exo</sub> –N	N–B <sub>endo</sub>	B <sub>exo</sub> –O	H–C
	B3LYP/6-31G*							
(R)	–22.9	169.3	1.448	1.614	1.596	1.611	1.559	1.097
(S)	–100.4	173.9	1.446	1.610	1.606	1.610	1.553	1.094
	HF/3-21G							
(R)	–31.3	–179.4	1.455	1.580	1.616	1.625	1.575	1.082
(S)	–89.3	154.8	1.453	1.580	1.619	1.623	1.569	1.078
	AM1							
(R)	–6.6	156.8	1.436	1.672	1.583	1.591	1.606	1.127
(S)	–121.3	165.4	1.439	1.672	1.590	1.589	1.607	1.129

<sup>a</sup> Interatomic distances are in Å, and angles, in deg. B<sub>exo</sub>–H and C–H indicate the interatomic distances involving the hydride nearest to the carbonyl group.

increasingly less exothermic as the level of the calculation improves. Of course, for a better description of the process, solvation should be included. This subject will be covered in a future publication.

In general the reaction is energetically favored but entropically disfavored. The reaction internal energy at the B3LYP/6-31G\* level is less favorable than at the HF/3-21G and AM1 levels because the last two methods overestimate the B••O interaction in both complexes and products.

**Remarks about Computational Aspects in the Modeling of CBS Reductions.** The complexation of the ketone to CBS–



BH<sub>3</sub> is not easily modeled, and probably the modeling of the whole mechanism depends heavily on the substrate as well as on the level of theory. The most difficult aspect indeed in the computational modeling of CBS reductions is the B••O interaction. Its nature is essentially electrostatic and involves the B atom vacant p orbital and one of the carbonyl O lone pairs. An exploratory decomposition of the interaction energy in the Kitaura and Morokuma framework,<sup>64</sup> carried out for the exo/anti complex at the HF/3-21G level, considering the CBS–BH<sub>3</sub> and PhMK partners in the adduct geometry, produced electrostatic and charge transfer terms of –65.46 and –33.08 kcal/mol, respectively, thus indicating that there is also a sensitive charge transfer contribution, as expected.

As it could be derived from the results presented in this paper, and primarily from those concerning acetophenone–CBS–BH<sub>3</sub> complexes, different pictures are obtained, depending on the level of theory adopted, for three main reasons. Some of the differing features between the AM1 results on one side and HF and DFT results on the other have already been discussed. Concerning the dependence of the description of the B••O interaction on the method adopted, there are a few remarks that are worth mentioning, though the topic has been discussed in more detail elsewhere.<sup>36</sup>

First of all, as largely known, the electrostatic contribution to the energy is overestimated at the HF/3-21G level, causing exceedingly favorable complexation energies and too short B••O equilibrium distances.

Second, BSSE, which is an artifact whose magnitude depends on the basis set and on the method, plays an important role. Due to the large deformation of both the oxazaborolidine and the ketone upon complexation, geometry changes must be taken into account and excluded from the CP correction.

At the HF/3-21G level, exo/anti, skew/anti, and skew/syn complex geometries are minimum energy structures. Moreover, their internal energies of complexation are negative (favorable). Conversely, when the entropic contribution is included, the complexation free energy increases by ~20 kcal/mol, and positive values are obtained (Table 5). This means that even the HF/3-21G level, which overestimates the B••O interaction, predicts a nonspontaneous complexation, although higher energy structures of the aforementioned conformations may be local minima with a short but finite lifetime, and not transient intermediates. The results differ when using DFT methods. Calculations at the B3LYP/3-21G level describe the exo/syn complex as a stable structure, while the skew/anti one is again produced instead of the endo/anti geometry. The outcome is analogous to that using the same basis set with another DFT functional, MPW1PW91. As in case of the calculations at the HF/3-21G level, DFT calculations carried out with the 3-21G basis set are apparently affected by a large BSSE. At the HF/6-31G\* level, the overestimate of the electrostatic contribution to the interaction energy as well as BSSE is reduced, but in this case, no complex conformation is found to be a minimum energy structure.

This suggests that at least a fraction of electron correlation should be included to satisfactorily describe the system. The B3LYP functional gives results that are close to MP2 but at a lower computational cost.<sup>36</sup> For these reasons, B3LYP/3-21G calculations appear to be more reliable than the HF/3-21G ones in the rationalization of the key steps of CBS reductions.

Furthermore, the B3LYP/6-31G\* level represents an even better choice, when it is affordable. Nonetheless, also calculations at lower levels, such as AM1 or HF/3-21G, are worth being considered, because the comparisons can yield interesting results. According to B3LYP/6-31G\* calculations on acetophenone–CBS–BH<sub>3</sub>, only skew/anti and exo/anti geometries are local minima. Their complexation energy is positive even without considering the entropic contribution to the free energy, though they are local minima with an energy barrier to dissociation.

The collected data seem to indicate that exo/syn- and endo/anti-like TS's can be reached through pathways in which the relevant "complexes" are transient species; the TS's might be reached directly when the two partners approach each other from infinite distance or, more likely, passing first through complexes with exo/anti or skew/anti conformations, which are local minima, though less stable than separate acetophenone and CBS–BH<sub>3</sub>. By means of rotations about the C–B–O–C and B–O–C–Ph dihedrals, as well as by inversion of the B–O–C angle, a complex geometry may be converted into another. If any energy barriers for these interconversions exist, their height is not known, although some information can be inferred from the work done by Wiberg and LePage on some very small model systems.<sup>67</sup>

Whether a particular geometry is stable or not depends on the repulsive interaction between the catalyst and the substrate R<sub>L</sub> and R<sub>S</sub> groups, which varies according to their mutual spatial disposition and to the nature of R<sub>L</sub> and R<sub>S</sub> themselves. For this reason, the observations made on the reduction of acetophenone will not necessarily hold when studying the reduction of different systems. Actually, in modeling the CBS reduction of methyl  $\alpha$ -methoximino- $\beta$ -keto-butyrate (either in the (Z) or the (E) configuration), the exo/syn complex was characterized at the HF/3-21G level as a local minimum.<sup>69</sup> The correct description of repulsive interactions, greatly destabilizing certain complex geometries with respect to others and even with respect to the isolated species, has been shown to depend on an adequate choice of method and level of calculations.

**Prediction of the Stereochemical Outcome in the Reduction of Acetophenone.** Free energy results allow the prediction, at least on a qualitative basis, of the outcome of a reaction that might yield different products as a consequence of the existence of two or more reaction paths.

In the presence of competing reaction paths, the main factors determining the outcome of a reaction are the energies of reactants and products, when the reaction is reversible, or that of the TS's, when the reaction is irreversible, as described in Eyring's transition state theory (TST).<sup>70</sup>

A rigorous prediction of the stereochemical outcome would require a more complex approach than just examining transition state free energies, and of course it would require much more complex calculations. Some examples of further refinement include the explicit calculation of the partition functions for

(69) Tomasi, S. Applications for Oxazaborolidine-Catalysed Reductions: a Theoretical and Experimental Study of the Double Diastereoselective Reduction of Protected  $\alpha$ -Oximino- $\beta$ -keto Esters, Ph.D. Thesis, University of Pisa, 2002.

(70) (a) Eyring, H. J. *Chem. Phys.* **1935**, *3*, 107. (b) Evans, M. G.; Polanyi, M. *Trans. Faraday Soc.* **1935**, *31*, 875. (c) Wigner, E. *Trans. Faraday Soc.* **1938**, *34*, 875. (d) Eyring, H.; Wynne-Jones, W. F. K. *J. Chem. Phys.* **1935**, *3*, 492. (e) Jensen, F. *Introduction to Computational Chemistry*; Wiley: New York, 1999; Chapter 12, pp 247–308.

**Table 9.** Enantiomeric Excess Values Predicted at the AM1, HF/3-21G, and B3LYP/6-31G\* Levels Compared to the Experimental Value<sup>1 a</sup>

	AM1	HF/3-21G	B3LYP/6-31G*	experimental
[R]/[S]	51	114	206	66
ee %	96	98	99	97

<sup>a</sup> In all cases, the reported values refer to (*R*)-1-phenylethanol.

anharmonic vibrations and internal rotations, the introduction of temperature dependence through the inclusion of entropy effects, in order to generate a free energy instead of a potential energy surface (variational transition state theory, VTST), and the evaluation of recrossings and tunneling in order to produce a transmission coefficient. For the numerous reactions occurring in solution, if high quality results are sought, solvation is another very important factor that needs to be considered, whose modeling is quite a challenging task, making the calculations even more cumbersome. Though resorting to very refined methods, theoretical calculations are not always capable of accurately predicting absolute reaction rates. Nonetheless, in the case of competing pathways for a given reaction, all with the same mechanism, errors affecting a reaction rate calculation are very similar to those affecting the others, so that relative rate calculations can effectively be carried out.

In the specific framework of enantioselective ketone reductions with borane, catalyzed by a chiral oxazaborolidine, it has been shown that the product is obtained after a series of steps of the catalytic cycle, in which the crucial moment for enantioselection is the hydride transfer. This particular step is highly exothermic and, therefore, virtually irreversible. Thus, an approximate prediction of enantiomeric excess, that is, the ratio of the two enantiomers produced in the process, can be done from the transition state free energies of the competing reaction pathways, according to the fundamental equation of TST, which at a given temperature *T* relates the reaction rate constant, *k*, exclusively to the free energy of the transition state:

$$k = \frac{k_B T}{h} \exp(-G_{\text{rel}}^\ddagger/RT) \quad (1)$$

where  $G_{\text{rel}}^\ddagger$  indicates the free energy difference between the transition state and an arbitrarily chosen reference energy (in this case, that of the PhMK-CBS-BH<sub>3</sub> complex of the *exo/anti* conformation). The constants *h* and *k<sub>B</sub>* are Planck's constant and Boltzmann's constant, respectively. Actually, the TST expression really holds if all the molecules that pass over the transition state go on to the product. To allow "recrossings", where a molecule that reaches the transition state instead of going to the products goes back to the reactant, a transmission factor coefficient  $\kappa$  is sometimes introduced. This factor also accounts for the phenomenon of tunneling, but in most cases, as here, it is considered to be close to one. This approach was successfully used also to determine the regioisomeric ratio between branched and linear aldehydes in the hydroformylation of vinyl substrates.<sup>71</sup>

Therefore, the ratio between the products having (*R*) and (*S*) configuration is given by the ratio between the rate of the *exo/anti* pathway and the combined rates of the *exo/syn* and *endo/*

*anti* pathways. The temperature dependent pre-exponential factor is simplified, and only the exponential parts are retained:

$$\frac{[R]}{[S]} = \frac{\exp(-G_{\text{rel}(\text{exo/anti})}^\ddagger/RT)}{\exp(-G_{\text{rel}(\text{exo/syn})}^\ddagger/RT) + \exp(-G_{\text{rel}(\text{endo/anti})}^\ddagger/RT)} \quad (2)$$

The enantiomeric excess can be calculated as follows:

$$ee\% = \frac{[R] - [S]}{[R] + [S]} \cdot 100 = \frac{\frac{[R]}{[S]} - 1}{\frac{[R]}{[S]} + 1} \cdot 100 \quad (3)$$

Application of eqs 2 and 3 to the results obtained from calculations at the AM1, HF/3-21G, and B3LYP/6-31G\* levels of theory produced the surprisingly good results reported in Table 9.

The calculated enantiomeric excesses reflect the quality of the calculated transition states, giving confidence that the method developed for transition state characterization in the oxazaborolidine-catalyzed reduction of acetophenone could be successfully applied also to substrates not yet experimentally studied.

## Conclusions

The computational work on the CBS-catalyzed reduction of acetophenone has been carried out by means of a variety of methods (AM1, HF, and DFT), allowing a better insight into the origin of stereoselectivity in this type of reactions.

Some (*exo/anti*, *exo/syn*, and *endo/anti*) of the conceivable reactant complexes as well as two skew conformations (*skew/syn* and *skew/anti*) were found stable at the AM1 level. On the contrary, none of them were located at the HF/6-31G\* level, while at least three of them (*exo/anti*, *skew/syn*, and *skew/anti*) resulted in being stable at the HF/3-21G level, which is known to overestimate electrostatic interactions and is prone to BSSE. Both the *exo/syn* and *endo/anti* starting structures evolved in the optimization to a *skew/anti* conformation. A similar behavior was observed at the B3LYP/6-31G\* level that, however, did not produce any *skew/syn* conformation. The 3-21G basis set sharply overestimated the conformer stability also coupled to different density functionals, such as B3LYP and MPW1PW91, where an *exo/syn* conformer was found to be stable as well. Since the inclusion of correlation corrections was not sufficient to counterbalance its faults, the DFT/3-21G levels were left aside and the subsequent investigation was carried out with AM1 and at the HF/3-21G and B3LYP/6-31G\* levels.

An accurate and systematic search for transition states has been performed by developing an efficient and reliable strategy, which has been successfully used also for the search of transition states in reactions involving different substrates and oxazaborolidine catalysts.

Though considerable differences concerning the existence itself of CBS-BH<sub>3</sub>-acetophenone adducts emerged among the various methods, the overall picture of the reduction reaction was fairly maintained, taking into account either internal or free energies, even though thermal corrections considerably destabilize the relevant complexes.

The free energy results obtained have been employed for predicting the stereochemical outcome: the experimental values of stereoselectivity in the CBS reduction of acetophenone have been accurately reproduced, suggesting that the method developed can be successfully exploited to predict the stereoselectivity in reductions of compounds not yet carried out experimentally.

(71) Alagona, G.; Ghio, C.; Lazzaroni, R.; Settambolo, R. *Organometallics* **2001**, *20*, 5394.